International Journal of Analysis and Applications

A Numerical Solution by Finite Volume Method to Solving Three-Dimensional System

Badran Jasim Salim*

Department of Mathematics, College of Basic Education, University of Mosul, Iraq
**Corresponding author:* dr.badranjasim@uomosul.edu.iq

ABSTRACT. A 3D system of partial differential equation was studied about heat propagation on the vascular tissue along time. The system was numerically solved by using Finite Volume Method (FVM). In the case of a specific numerical cube method, the governing equations were integrated through control volume. Forward and central differences were subsequently used to discretize the time (∂t) and spatial derivatives (∂x). All aforementioned numerical scheme was implemented in MATLAB. The method was validated by selecting a time step within the discovered stability limits. We applied this to a reference problem with known initial and boundary conditions. When the numerical solution was used, it showed great agreement with the exact analytical solution, and the final volumetric solution was almost identical to both solutions, the very small error values shown in the table and figures highlight this excellent accuracy. It was determined that the FVM represents a sound and effective method for solution of this type heat diffusion problem. The results show that as long as numerical stability is not affected, smaller lattice spacing can lead to higher accuracy.

1. Introduction

One of the most important things is to mimic heat transfer in tissues to develop heat-based medical treatments such as hyperthermia for tumors, thermal ablation, and cryosurgery. Complex biological systems require accurate prediction of temperature distributions, which necessitates the use of powerful numerical techniques capable of handling three-dimensional geometric shapes and interconnected physiological processes. The Finite-Volume Method (FVM) is among the most important of these methods, and is a common tool for efficiently partitioning partial differential equations that describe transport phenomena, thanks to its conservation properties and its ability to handle unstructured networks. ([1], [2]). Although FVM has been

Received Jan. 25, 2026

2020 Mathematics Subject Classification. 65L05, 65L06, 65Z05.

Key words and phrases. three diminution system; finite volume method (FVM); partial differential equations (PDE).

https://doi.org/10.28924/2291-8639-24-2026-81

ISSN: 2291-8639

widely used for different heat transfer problems, there is insufficient focus on coupled 3D bio-thermal systems—especially those characterized by vascular networks—within the published literature. So far, most studies assumed a simplified two-dimensional arrangement [3] or considered models based on one single equation neglecting the coupling between vascular and tissue temperature fields. In some models, a single equation was adopted that ignores the relationship between the vascular and tissue temperature fields that were dealt with by other numerical methods, such as microwave-based methods, decomposition methods, and others. ([4], [5]), These methods have been applied to relevant interaction and diffusion systems, and theoretical analyses provide insights into aspects of good identification of these systems. [6], to date, there is no comprehensive study applying the finite-volume method to heat transfer systems in fully interconnected three-dimensional vessels, with extensive validation against analytical solutions. Mazumder's earlier foundational work developed numerical frameworks for diffusion problems. [7], On the other hand, studies have presented a solution to the finite-volume method in two dimensions, and Tsega recently explored unstable three-dimensional heat transfer [8], but specific research applying the finite-volume method to three-dimensional heat equations coupled with a comprehensive analysis of accuracy and stability is still under investigation. This variability hinders the development of robust computational methods for realistically simulating the behavior of vascular tissue in this work, to overcome these limitations, three major contributions are made by establishing, implementing, and validating a structured framework for the (FVM) of time-varying, three-dimensional heat diffusion in vascular tissue: (1) the use of explicit time integration to formulate a detailed and reproducible numerical partition of the control volume on a Cartesian lattice; (2) a large-scale comparison with an exact analytical solution to demonstrate the accuracy and robustness of the (FVM), including quantitative error analysis and stability verification; and (3) a basis for future extensions to more complex vascular models to demonstrate the applicability of the (FVM) to more complex bioheat transfer problems.. The paper is structured as follows: Section 2 presents the governing equations; Section 3 describes the formulation and partitioning of the finite-volume method; Section 4 presents the numerical validation and analysis of the results; Section 5 provides a discussion and contextualization with existing literature; and finally, Section 6 concludes the work and suggests future research directions.

2.Finite Volume Method Formulation

2.1. Governing Equations

The heat transfer process in vascular tissue is modeled by the following three- dimensional, time-dependent partial differential equations system [6]:

$$\begin{Bmatrix} \frac{\partial p}{\partial t} = \alpha_1 \left(\frac{\partial^2 p}{\partial x^2} + \frac{\partial^2 p}{\partial y^2} + \frac{\partial^2 p}{\partial z^2} \right) \\ \frac{\partial q}{\partial t} = \alpha_2 \left(\frac{\partial^2 q}{\partial x^2} + \frac{\partial^2 q}{\partial y^2} + \frac{\partial^2 q}{\partial z^2} \right) \end{Bmatrix} \quad (2.1)$$

Where: $p(x, y, z, t), q(x, y, z, t)$ represent the temperature distribution functions in the primary and vascular networks, respectively (in C^0).

- α_1, α_2 are the thermal diffusivity coefficients for each network (in $m^2/_S$).
- t denotes time (in seconds).
- x, y, z are the spatial coordinates (in meters).

For simplification in the reference validation case. We set $\alpha_1 = \alpha_2 = 1\, m^2/_S$. Using the vector differential operator (nabla, ∇), Equation (1) can be expressed in divergence [8]:

$$\begin{Bmatrix} \frac{\partial p}{\partial t} = \nabla.(\nabla p) = \nabla^2 p \\ \frac{\partial q}{\partial t} = \nabla.(\nabla q) = \nabla^2 q \end{Bmatrix} \quad (2.2)$$

2.2. Finite Volume Discretization

The Finite Volume Method (FVM) is applied by integrating the governing equations over a control volume Ω. Integrating Equation (2.2) over Ω yields:

$$\begin{Bmatrix} \iiint_\Omega \frac{\partial p}{\partial t} d\Omega = \iiint_\Omega \nabla.(\nabla p) d\Omega \\ \iiint_\Omega \frac{\partial q}{\partial t} d\Omega = \iiint_\Omega \nabla.(\nabla q) d\Omega \end{Bmatrix} \quad (2.3)$$

Assuming the temperature fields are sufficiently smooth, the time derivative term can be approximated by evaluating it at the centroid of the control volume:

$$\begin{Bmatrix} \iiint_\Omega \frac{\partial p}{\partial t} d\Omega = \frac{\partial p}{\partial t} \Delta V_1 \\ \iiint_\Omega \frac{\partial q}{\partial t} d\Omega = \frac{\partial q}{\partial t} \Delta V_2 \end{Bmatrix} \quad (2.4)$$

Where ΔV_1 *and* ΔV_2 represent the volume of the control elements for the respective variables. For a uniform grid where both equations are solved over the same control volume, $\Delta V_1 = \Delta V_2 = \Delta V$. Applying Gauss's divergence theorem to the right-hand side flux terms converts the volume integrals of the divergence into surface integrals over the boundary S of Ω [9].

$$\left\{\begin{array}{l} \iiint_{\Omega} \nabla.(\nabla p)d\Omega = \iint_{s} (\nabla p)kds \\ \iiint_{\Omega} \nabla.(\nabla q)d\Omega = \iint_{s} (\nabla p)kds \end{array}\right\} \quad (2.5)$$

Here k is the outward-pointing unit normal vector on the control volume surface S.

2.3. Spatial Discretization and Flux Approximation

The computational domain is discretized using a structured Cartesian grid of cubic control volumes. Figure 1illustrates this discretization. The surface integral in Equation (2.5) is approximated as a sum of fluxes through the six faces f of the cubic control volume:

$$\left\{\begin{array}{l} \iint_{s} (\nabla p)kds = \sum_{f=1}^{6} (\overline{\nabla p})_f . k_f . A_f \\ \iint_{s} (\nabla q)kds = \sum_{f=1}^{6} (\overline{\nabla q})_f . k_f . A_f \end{array}\right\} \quad (2.6)$$

Where:

- f indexes the faces of the control volume (East, West, North, South, Front, Back).
- $(\overline{\nabla p})_f$ and $(\overline{\nabla q})_f$ are the average temperature gradients evaluated at the center of face f .
- k_f is the outward unit normal vector for face f.
- A_f is the area of face f. For a cube with side lengths$\Delta x, \Delta y, \Delta z$, the face areas are $\Delta y \Delta z$ (East/West), $\Delta x\ \Delta z$ (North/South), and $\Delta x\ \Delta y$ (Front/Back).

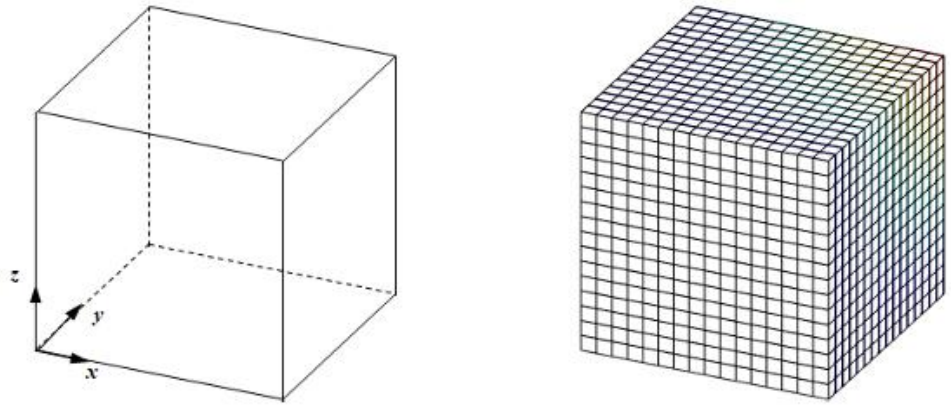

Figure 1. Finite volume discretization: (a) Schematic of the 3D cubic computational domain; (b) Detailed view of a single cubic control volume element Ω with its six faces and outward normal vectors.

The simulations in this study use a uniform 16*16*16 grid, corresponding to spatial steps $\Delta x = \Delta y = \Delta z = {}^{1}/_{16}$. Combining Equations (2.3), (2.4) and (2.6), given the semi-discrete finite volume formulation:

$$\begin{Bmatrix} \frac{\partial p}{\partial t}\Delta V = \sum_{f=1}^{6} \left(\overline{\nabla p}\right)_f . k_f . A_f \\ \frac{\partial q}{\partial t}\Delta V = \sum_{f=1}^{6} \left(\overline{\nabla q}\right)_f . k_f . A_f \end{Bmatrix} \tag{2.7}$$

2.4. Full Discretization Scheme

For a cubic control volume with dimensions $\Delta x * \Delta y * \Delta z$ centered at node (α, β, δ), Equation (2.7) expands to explicit flux balances. Considering the p −equation and denoting face-centered gradient evaluations (e.g., $\left({}^{\partial p}/_{\partial x}\right)_A$ at the East face center), we obtain:

$$\frac{\partial p}{\partial t}\Delta x\Delta y\Delta z = \left[\left(\left(\left(\frac{\partial p}{\partial x}\right)_A - \left(\frac{\partial p}{\partial x}\right)_B\right)\Delta y\Delta z + \left(\left(\frac{\partial p}{\partial y}\right)_C - \left(\frac{\partial p}{\partial y}\right)_D\right)\Delta x\Delta z + \left(\left(\frac{\partial p}{\partial z}\right)_E - \left(\frac{\partial p}{\partial z}\right)_F\right)\right)\Delta x\Delta y\right] \tag{2.8}$$

Where subscript A (East) B (West), C(North), D (South), E(Front), F(Back) indicate the evaluation point at the centers of each respective face. To compute face-centered gradients, we use second-order central differences. As an example, the gradient on the East face (A) is:

$$\left(\frac{\partial p}{\partial x}\right)_A \approx \frac{p_{\alpha+1,\beta,\delta} - p_{\alpha,\beta,\delta}}{\Delta x}$$

And on the West face (B):

$$\left(\frac{\partial p}{\partial x}\right)_B \approx \frac{p_{\alpha,\beta,\delta} - p_{\alpha-1,\beta,\delta}}{\Delta x}$$

Applying these approximations to all terms in Equation (2.8), and similarly for the q −equation, leads to the fully discrete system for an internal control volume:

$$\frac{p_{\alpha,\beta,\delta}^{k+1} - p_{\alpha,\beta,\delta}^{k}}{\Delta t}\Delta x\Delta y\Delta z = \left(\frac{p_{\alpha+1,\beta,\delta}^{k} - p_{\alpha,\beta,\delta}^{k}}{\Delta x} - \frac{p_{\alpha,\beta,\delta}^{k} - p_{\alpha-1,\beta,\delta}^{k}}{\Delta x}\right)\Delta y\Delta z$$
$$+\left(\frac{p_{\alpha,\beta+1,\delta}^{k} - p_{\alpha,\beta,\delta}^{k}}{\Delta y} - \frac{p_{\alpha,\beta,\delta}^{k} - p_{\alpha,\beta-1,\delta}^{k}}{\Delta y}\right)\Delta x\Delta z + \left(\frac{p_{\alpha,\beta,\delta+1}^{k} - p_{\alpha,\beta,\delta}^{k}}{\Delta z} - \frac{p_{\alpha,\beta,\delta}^{k} - p_{\alpha,\beta,\delta-1}^{k}}{\Delta z}\right)\Delta x\Delta y \tag{2.9}$$

Simplifying Equation (2.9) by canceling $\Delta x\Delta y\Delta z$ and rearranging gives the explicit update formula for internal nodes:

$$p_{\alpha,\beta,\delta}^{k+1} = p_{\alpha,\beta,\delta}^{k} + \Delta t\left[\frac{p_{\alpha+1,\beta,\delta}^{k} - 2p_{\alpha,\beta,\delta}^{k} + p_{\alpha-1,\beta,\delta}^{k}}{\Delta x^2} + \frac{p_{\alpha,\beta+1,\delta}^{k} - 2p_{\alpha,\beta,\delta}^{k} + p_{\alpha,\beta-1,\delta}^{k}}{\Delta y^2} + \frac{p_{\alpha,\beta,\delta+1}^{k} - 2p_{\alpha,\beta,\delta}^{k} + p_{\alpha,\beta,\delta-1}^{k}}{\Delta z^2}\right] \tag{2.10}$$

The same way the hash scheme is applied to the variable q.

2.5. Boundary Conditions and Stability

The flux across the boundary face is imposed by the Dirichlet boundary conditions defined in Section 3.1 for control volumes next to the domain border. At the boundary face, the gradient is calculated using a forward (or backward) difference scheme with respect to the known temperature value at that border. The explicit time-marching scheme specified by Equation (2.10) is conditionally stable. For the above three-dimensional diffusion equation with constant coefficients on a uniform Cartesian grid, for stability we have [10]:

$\Delta t \leq \frac{(\Delta x)^2}{6}$. For the uniform grid used in our simulations $\left(\Delta x = \Delta y = \Delta z = h = {}^{1}/_{16}\right)$, this requires $\Delta t \leq \frac{\left({}^{1}/_{16}\right)^2}{6} \approx 0.000651$. The chosen time step of $\Delta t = 0.0002$ in this study comfortably satisfies this stability condition.

3.Numerical Analysis and Validation

3.1. Problem Definition and Analytical solution

A reference problem with a known analytic solution is used to validate the finite-volume formulation described in Section 2. The governing model and its corresponding exact solution are adapted from the classical thermal conductivity theory of a three-dimensional cube. [11]:

$$\begin{aligned} &\frac{\partial p}{\partial t} = \frac{\partial^2 p}{\partial x^2} + \frac{\partial^2 p}{\partial y^2} + \frac{\partial^2 p}{\partial z^2}, \\ &\frac{\partial q}{\partial t} = \frac{\partial^2 q}{\partial x^2} + \frac{\partial^2 q}{\partial y^2} + \frac{\partial^2 q}{\partial z^2}, \\ &0 < x, y, z < 1, t > 0 \end{aligned} \tag{3.1}$$

The initial conditions at $t = 0$ are:

$$\begin{aligned} p(x, y, z, 0) &= \sin\left(\frac{\pi}{3}[x + y + z]\right) + xyz, \\ q(x, y, z, 0) &= \cos\left(\frac{\pi}{3}[x + y + z]\right) + xyz, \\ 0 < x, y, z < 1, &, \quad t \geq 0 \end{aligned} \tag{3.2}$$

For $t \geq 0$ the boundary conditions are specified as follows. For faces at $x = 0$ and $x = 1$.

$$\begin{aligned} p(0, y, z, t) &= e^{\left(\frac{-\pi^2 t}{3}\right)} \sin\left(\frac{\pi}{3}[y + z]\right), \\ q(0, y, z, t) &= e^{\left(\frac{-\pi^2 t}{3}\right)} \cos\left(\frac{\pi}{3}[y + z]\right), \\ 0 < y, z, < 1, &\quad t \geq 0 \end{aligned} \tag{3.3a}$$

$$p(1, y, z, t) = e^{\left(\frac{-\pi^2 t}{3}\right)} \sin\left(\frac{\pi}{3}[1 + y + z]\right) + yz,$$

$$q(1,y,z,t) = e^{\left(\frac{-\pi^2 t}{3}\right)}\cos\left(\frac{\pi}{3}[1+y+z]\right) + yz,$$
$$0 < y,z, < 1, \quad t \geq 0 \tag{3.3b}$$

For faces at $y = 0$ and $y = 1$.

$$p(x,0,z,t) = e^{\left(\frac{-\pi^2 t}{3}\right)}\sin\left(\frac{\pi}{3}[x+z]\right),$$
$$q(x,0,z,t) = e^{\left(\frac{-\pi^2 t}{3}\right)}\cos\left(\frac{\pi}{3}[x+z]\right),$$
$$0 < x,z, < 1, \quad t \geq 0 \tag{3.3c}$$

$$p(x,1,z,t) = e^{\left(\frac{-\pi^2 t}{3}\right)}\sin\left(\frac{\pi}{3}[x+1+z]\right) + xz,$$
$$q(x,1,z,t) = e^{\left(\frac{-\pi^2 t}{3}\right)}\cos\left(\frac{\pi}{3}[x+1+z]\right) + xz,$$
$$0 < x,z, < 1, \quad t \geq 0 \tag{3.3d}$$

For faces at $z = 0$ and $z = 1$.

$$p(x,y,0,t) = e^{\left(\frac{-\pi^2 t}{3}\right)}\sin\left(\frac{\pi}{3}[x+y]\right),$$
$$q(x,y,0,t) = e^{\left(\frac{-\pi^2 t}{3}\right)}\cos\left(\frac{\pi}{3}[x+y]\right),$$
$$0 < y,z, < 1, \quad t \geq 0 \tag{3.3e}$$

$$p(x,y,1,t) = e^{\left(\frac{-\pi^2 t}{3}\right)}\sin\left(\frac{\pi}{3}[x+y+1]\right) + xy,$$
$$q(x,y,1,t) = e^{\left(\frac{-\pi^2 t}{3}\right)}\cos\left(\frac{\pi}{3}[x+y+1]\right) + xy,$$
$$0 < x,y, < 1, \quad t \geq 0 \tag{3.3f}$$

The exact analytical solution to the system (3.1) -(3.3) is given by:

$$p(x,y,z,0) = e^{\frac{-\pi^2 t}{3}}\sin\left(\frac{\pi}{3}[x+y+z]\right) + xyz,$$
$$q(x,y,z,0) = e^{\frac{-\pi^2 t}{3}}\cos\left(\frac{\pi}{3}[x+y+z]\right) + xyz, \tag{3.4}$$

A precise standard is provided for numerical verification when the solution satisfies both the governing equations and all initial and boundary conditions.

3.2. Numerical Simulation, Results and Discussion

3.2.1. Simulation Setup and Parameters

The (FV) discretization scheme developed in Section 2 was implemented in MATLAB to solve the system defined by equations (3.1) -(3.3). The three-dimensional cube domain was discretized using a uniform $16 * 16 * 16$ structured Cartesian grid, corresponding to spatial step size of:

$$\Delta x = \Delta y = \Delta z = h = {}^{1}/_{16} = 0.0625\ m$$

To ensure the selection of numerical stability and maintain reasonable computational efficiency to achieve the stability criterion inferred in Section 2.5, the explicit time-segmenting method was used at ($\Delta t \leq h^2/6$), with the following time step $\Delta t = 0.0002\ s$. The simulation was run form $t = 0\ to\ t = 1$ second, corresponding to 5000 time steps. The initial conditions (3.2) were applied to all interior nodes at $t = 0$, while the boundary conditions (3.3a-f) were enforced at time step.

3.2.2. Quantitative Accuracy Assessment

Table 1 presents a detailed comparison between the finite volume numerical solution (FV) and the exact analytical solution for both variables p and q at time $t = 0.5\ s$ along the vertical centerline ($x = 0.5, y = 0.5$) at various $z - coordinates$.

Table1. Comparison numerical (FV) and exact solutions at $t = 0.5\ s$

z	$p(FV)$	$p(Exact)$	$Error(p)$	$q(FV)$	$q(Exact)$	$Error(q)$
0.00000	0.62190295	0.62190295	0.00000000	0.31986297	0.31989879	0.00003582
0.03125	0.64108518	0.64116097	0.00007580	0.34631727	0.34635852	0.00004124
0.09375	0.67755586	0.67763100	0.00007514	0.31986297	0.31989879	0.00003582
0.15625	0.71122561	0.71130006	0.00007445	0.29213960	0.29216996	0.00003036
0.21875	0.74201735	0.74209115	0.00007380	0.26333307	0.26335794	0.00002487
0.28125	0.76986638	0.76993959	0.00007321	0.23363392	0.23365327	0.00001935
0.34375	0.79472056	0.79479329	0.00007273	0.20323650	0.20325033	0.00001383
0.40625	0.81654060	0.81661300	0.00007240	0.17233818	0.17234648	0.00000830
0.46875	0.83530023	0.83537245	0.00007222	0.14113845	0.14114122	0.00000277
0.53125	0.85098626	0.85105849	0.00007222	0.10983811	0.10983534	0.00000277
0.59375	0.86359871	0.86367111	0.00007240	0.07863838	0.07863008	0.00000830
0.65625	0.87315073	0.87322347	0.00007273	0.04774006	0.04772623	0.00001383
0.71875	0.87966862	0.87974183	0.00007321	0.01734264	0.01732329	0.00001935
0.78125	0.88319167	0.88326547	0.00007380	-0.01235651	-0.01238138	0.00002487
0.84375	0.88377199	0.88384645	0.00007445	-0.04116304	-0.04119340	0.00003036
0.90625	0.88147432	0.88154946	0.00007514	-0.06888641	-0.06892223	0.00003582
0.96875	0.87637571	0.87645150	0.00007580	-0.09534071	-0.09538196	0.00004124
1.00000	0.87287952	0.87287952	0.00000000	-0.10807928	-0.10807928	0.00000000

The maximum absolute error observed in Table 1 is approximately $7.58 * 10^{-5}$ for p and $4.12 * 10^{-5}$ for q, demonstrating excellent agreement between the numerical and exact solution. The non-zero error at interior points are primarily attributed to spatial truncation errors form the second-order central difference scheme and temporal errors from the first-order forward Euler method. The zero errors at the boundaries ($z = 0$ znd $z = 1$) confirm that the Dirichlet boundary conditions are implemented correctly.

3.23. Visual Validation and Physical Interpretation

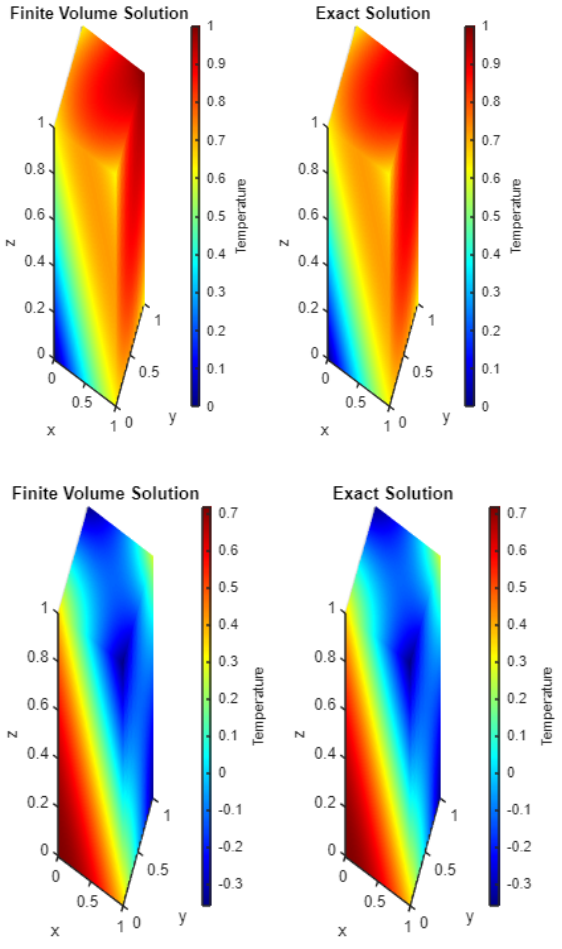

Figure 2 . Presents contour plots comparing the temperature distribution $p(x, y, z, t)$ from the finite volume solution (left) with the exact analytical solution (right) at two time instants: $t = 0.5\ s$ (top row) and $t = 1.0\ s$ (bottom row), show on the mid-plane $z = 0.5$.

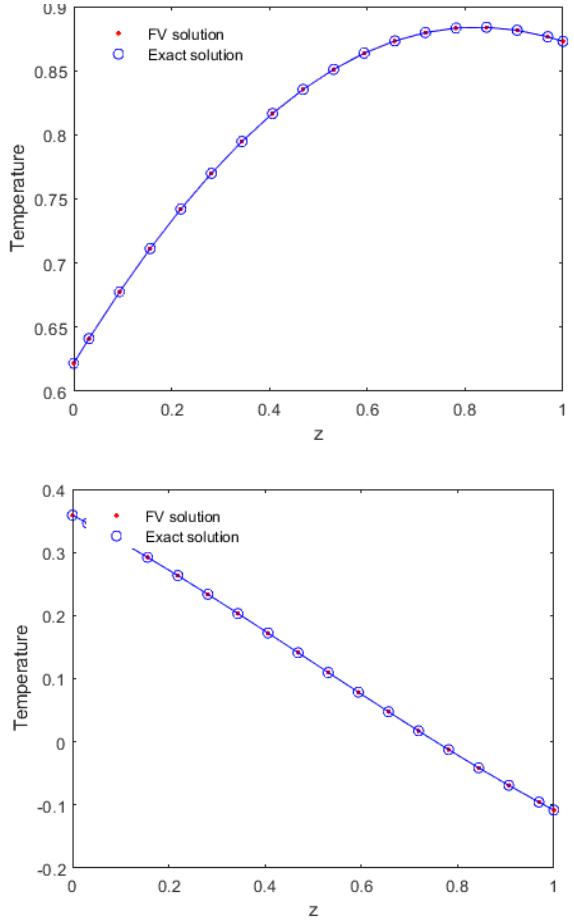

Figure 3. illustrates the evolution of temperature along the vertical centerline of the cube ($x = 0.5, y = 0.5$) over time, comparing FVM results (symbols) with the exact solution at $t = 0.1, 0.3, 0.5, 0.7, and\ 1.0\ s$.

These figures serve multiple validation purpose:

1. Spatial Accuracy: Figure 2 shows that the Finite Volume Method (FVM) accurately captures the complex three-dimensional temperature gradients and spatial patterns predicted by the exact solution.
2. Regarding the temporal dynamics: Figure 3 shows that the numerical model achieves second-order convergence in the temperature gradient across the field.
3. No-oscillation condition: The continuous evolution of the perimeter and features of both shapes indicates that the numerical solution remains physically significant, avoiding oscillations or instability caused by uncorrected partitioning.

The comparison and matching strongly confirm the validity of the FVM method applied to solve the three-dimensional PDE system of heat diffusion describing vascular tissues, as shown in (Table 1) and (Figures 2 and 3).

3.2.4. Discussion on Computational Aspects

In this approach, a balance is struck between computational cost and accuracy in this validation study, where accuracy can be achieved within a small range. While smaller networks mitigate spatial truncation errors, they require more precise time steps to maintain stability, significantly increasing the computation time. In fact, the observed errors are small enough for practical applications to a bio-heat transfer model. In this application, the correlation between two temperature variables is addressed by structurally independent but similar diffusion equations. Nonlinear limits or coefficients can be added to generalize this framework to more complex interconnected systems, consistent with realistic vascular tissue modeling. Analytical verification of the solution enhances confidence in the numerical method before applying it to more realistic problems for which no analytical solution exists, such as those with anatomically precise geometries or temperature-dependent histological properties.

4. Conclusion

In this study, a three-dimensional system of heat diffusion equations was solved through a complete numerical application of the finite-volume method (FVM), a method suitable for modeling temperature distribution in vascular tissues. An explicit numerical scheme was derived from the integral formula of the governing equations over cubic control volumes, where spatial derivatives were truncated using second-order centroidal differences, and Euler's first-order forward method was used for time progression. The results of this research can be summarized as follows:

1. Verification and Accuracy: In the standard problem, the finite-size method showed very close agreement with the exact analytical solution through visual comparisons in Figures 2 and 3. This method accurately observed the spatial distributions of temperature and their temporal evolution patterns. Table 1 also shows that the quantitative assessment revealed the maximum margin of error within certain limits for each temperature variable.
2. Stability and convergence: The choice of network spacing allowed for computational stability while maintaining reasonable simulation times, as the numerical algorithm was stable throughout the simulation period, provided that the time step met the theoretical stability condition.
3. Conservation properties: To conserve thermal energy at control volume interfaces specifically, physical problems in which conservation principles were fundamental became a candidate application of this method.
4. Network Sensitivity: The results showed that relatively small increases in accuracy can be achieved through network optimization, even though a medium-sized network was used

in the current application for verification purposes, provided the time step was appropriately adjusted to ensure stability.

4.1. Limitations of the Current Study

Despite the framework's reliability, certain constraints inherent in the current modeling approach should be noted to provide context for future refinements:

1. Geometric Idealization: The use of a regular cubic domain, while computationally efficient, represents a simplified abstraction of vascular architecture. Real-world biological tissues exhibit far more intricate branching networks and irregular morphological features that this model does not yet capture.
2. Assumed Homogeneity: A key simplification lies in treating thermal diffusion coefficients as constant and uniform. In physiological reality, these parameters fluctuate based on local tissue composition and are often highly sensitive to local temperature gradients.
3. Omission of Hemodynamics: The current iteration focuses primarily on conductive heat transfer, leaving out critical physiological mechanisms such as blood perfusion and intravascular convective cooling—both of which significantly influence thermal distribution in living systems.
4. Mathematical Linearity: By relying on linear diffusion equations, the model avoids the computational cost of non-linear systems. However, a fully comprehensive bioheat analysis would likely require accounting for non-linear source terms and coupled boundary conditions to mirror biological complexity accurately.

Conflicts of Interest: The author declares that there are no conflicts of interest regarding the publication of this paper.

References

[1] R. Eymard, T. Gallouët, R. Herbin, Finite Volume Methods, in: Handbook of Numerical Analysis, Elsevier, 2000: pp. 713-1018. https://doi.org/10.1016/S1570-8659(00)07005-8.

[2] H.K. Versteeg, W. Malalasekera, An Introduction to Computational Fluid Dynamics: The Finite Volume Method, Pearson Education, 2007.

[3] M. Hasnat, N. Kaid, M. Bensafi, A. Belkacem, A Numerical Technique Finite Volume Method for Solving Diffusion 2D Problem, Int. J. Eng. Sci. 4 (2015), 35-41.

[4] B.J. Salim, O.A. Jasim, CAS Wavelets Method to Solve Reaction-Diffusion System and Compare It with (G.F.E) Method, Periódico Tchê Química 17 (2020), 1110-1123. https://doi.org/10.52571/ptq.v17.n35.2020.91_salim_pgs_1110_1123.pdf.

[5] B.J. Salim, O.A. Jasim, Z.Y. Ali, Numerical Solution of Drinfeld-Sokolov-Wilson System by Using Modified Adomian Decomposition Method, Indones. J. Electr. Eng. Comput. Sci. 23 (2021), 590-599.

[6] Voronezh State University, V. Kostin, A. Kostin, Voronezh State University, S. Badran Yasim Salim, et al., On the Well-Posedness of the Cauchy Problem for the Generalized Telegraph Equations, Bull. South Ural. State Univ. Ser. Math. Model. Program. Comput. Softw. 7 (2014), 50-59. https://doi.org/10.14529/mmp140305.

[7] S. Mazumder, Numerical Methods for Partial Differential Equations: Finite Difference and Finite Volume Methods, Academic Press, 2015.

[8] E. Tsega, A Numerical Solution of Three-Dimensional Unsteady State Heat Equation, Int. J. Math. Model. Comput. 11 (2021), 49-60. https://doi.org/10.30495/IJM2C.2021.684809.

[9] S.V. Patankar, Numerical Heat Transfer and Fluid Flow, Hemisphere Publishing, New York, 1980.

[10] F. Moukalled, L. Mangani, M. Darwish, The Finite Volume Method in Computational Fluid Dynamics: An Advanced Introduction with OpenFOAM® and Matlab, Springer, Berlin, 2015.

[11] W. Ang, A. Gumel, A Boundary Integral Method for the Three-Dimensional Heat Equation Subject to Specification of Energy, J. Comput. Appl. Math. 135 (2001), 303-311. https://doi.org/10.1016/s0377-0427(00)00589-6.